퓨란이 도입된 비대칭 비풀러렌계 어셉터를 기반으로 하는 고분자 태양전지

홍승균 · 송창은*,** · 임은희†

경기대학교 화학과, *한국화학연구원, **한국과학기술연합대학원대학교(UST)
(2020년 6월 16일 접수, 2020년 7월 16일 수정, 2020년 7월 22일 채택)

Polymer Solar Cells based on a Furan-containing Asymmetric Nonfullerene Acceptor

Seunggyun Hong, Chang Eun Song*,**, and Eunhee Lim†

Department of Chemistry, Kyonggi University, 154-42 Gwanggyosan-ro, Yeongtong-gu, Suwon 16227, Korea
*Korea Research Institute of Chemical Technology (KRICT), 141 Gajeongro, Yuseong-gu, Daejeon 34114, Korea
**University of Science and Technology (UST), Daejeon 34113, Korea
(Received June 16, 2020; Revised July 16, 2020; Accepted July 22, 2020)

초록: 고분자 태양전지의 어셉터로 비접합된 전자 주는 thiophene-furan 중심과 전자 끄는 옥틸로다닌 말단 그룹으로 이루어진 비대칭 비풀러렌 단분자 TF-ORH가 설계되었다. TF-ORH은 Knoevenagel 축합과 스즈끼 짝지음 반응을 통해 합성되었다. TF-ORH는 소자 제작에 충분한 열 안정성 및 용해도를 나타냈다. 용액과 비교하여, TF-ORH 필름은 596 nm에서 최대 흡수를 가지는 장파장 이동된(J-aggregation) UV-Vis 흡수를 나타내었고, 이는 저밴드갭 고분자 도너인 PTB7-Th의 특성과 상호보완적이다. 퓨란의 도입으로 thiophene 유사체인 T2-ORH와 비교하여 분자 궤도 에너지 준위들은 높아졌다. 활성층으로서 PTB7-Th:TF-ORH 블렌드 필름을 사용하여 제작된 고분자 태양전지 소자는 0.88 V의 개방전압과 0.70 eV의 낮은 에너지 손실로 1.21%의 전력 변환 효율을 나타냈다.

Abstract: An asymmetric nonfullerene small molecule, TF-ORH, containing a nonfused electron-donating core of thiophene, furan and electron-withdrawing octylrhodanine (ORH) end groups was designed as an acceptor for polymer solar cells (PSCs). TF-ORH was synthesized *via* Knoevenagel condensation and the Suzuki coupling reaction. TF-ORH exhibited sufficient thermal stability and solubility for device fabrication. Compared to solution, TF-ORH film showed a red-shifted UV–Vis absorption with an absorption maximum at 596 nm (*J*-aggregation), which is complementary with that of the low bandgap polymer donor of poly[4,8-bis(5-(2-ethylhexyl)thiophen-2-yl)benzo[1,2-*b*:4,5-b']dithiophene-*co*-3-fluorothieno[3,4-b]thiophene-2-carboxylate] (PTB7-Th). The introduction of furan elevated the molecular orbital energy levels of TF-ORH compared to the thiophene analog, T2-ORH. Finally, a PSC fabricated using a PTB7-Th:TF-ORH blend film as the active layer exhibited a power conversion efficiency of 1.21% with an open-circuit voltage of 0.88 V and a small energy loss of 0.70 eV.

Keywords: organic solar cell, polymer solar cell, non-fullerene acceptor, asymmetrical structure.

Introduction

Polymer solar cells (PSCs) have considered as a renewable energy source owing to their advantages, which include low weight, flexibility, ease of processability, and low cost.[1-5] Much effort has been devoted to exploiting new donor and acceptor materials as well as to optimize device fabrication. From the standpoint of material synthesis, in recent years there has been a shift from using fullerene derivatives, such as [6,6]-phenyl-C_{61}-butyric acid methyl ester ($PC_{60}BM$), to using non-fullerene acceptors (NFAs) as acceptor materials. The use of NFAs solves key intrinsic drawbacks of fullerenes, which include difficult chemical structure modification, weak UV–vis absorption, fixed energy levels, low stability, and large energy losses (E_{loss}s). The relatively easy synthesis of NFAs with various molecular structures enables the control of their physical properties, allowing the development of various electron acceptors with desirable properties. These acceptors can be used for

highly efficient and stable PSCs for future practical applications.[6]

Acceptor–donor–acceptor (A–D–A)-type NFAs have been considered promising candidates for high efficiency PSC acceptors.[7,8] In particular, remarkable power conversion efficiencies (PCEs) more than 15% have been realized in devices using ladder-type fused ring electron acceptors (FREAs) with large π-conjugated cores including indacenodithiophene and indacenodithieno[3,2-b]thiophene.[9,10] Two representative A–D–A-structured low bandgap acceptors are IT-4F and Y6, both of which provide high efficiencies of >14% when combined with various wide bandgap polymer donors.[11] Various synthetic strategies have been used to adjust the chemical structure of NFAs with a view to maximizing PSC efficiency, including side-chain engineering and introduction of electron-rich or electron-poor substituents into the backbones. Recently, the development of asymmetric NFAs has made significant progress toward higher PCEs, with asymmetric NFAs showing superior performance to their symmetric counterparts.[12-15] Various NFAs with asymmetric cores, side-chains, and terminal groups have been designed;[16-18] however, most successful asymmetric NFAs have been based on asymmetric FREA cores. Possible reasons for the superiority of asymmetric NFAs are that their structures may give rise to stronger intermolecular interactions, higher electron mobility in the film, and higher charge carrier transport. For greater detail, refer to recent reviews on the structure and characteristics of high-efficiency asymmetric acceptors.[16] Meanwhile, thiophene analogs, such as selenophene,[19-21] thiazole,[22-24] and furan,[25-27] have been utilized to develop π-conjugated polymers and small molecules. Some of these thiophene analogs of furan or selenophene have recently been introduced into asymmetric NFAs.[28,29]

In this study, we applied the "asymmetric core" strategy to our previously reported A–D–A-type NFA, T2-ORH, containing a nonfused bithiophene core as an electron-donating (D) unit and octylrhodanine end groups as electron-accepting (A) units.[30] In the current work, one thiophene of the bithiophene core of T2-ORH was replaced with a furan moiety, resulting in a simple asymmetric NFA, TF-ORH, based on a nonfused thiophene-furan core. The synthesis and physical properties, including thermal, optical, and electrochemical properties, of TF-ORH were investigated in detail and a PSC was fabricated using TF-ORH and the low bandgap polymer donor poly[4,8-bis(5-(2-ethylhexyl)thiophen-2-yl)benzo[1,2-b:4,5-b']dithiophene-co-3-fluorothieno[3,4-b]thiophene-2-carboxylate] (PTB7-Th).

Experimental

Synthesis. The syntheses of octylrhodanine (ORH) and B-T-ORH (Scheme 1) were described in our previous literatures.[18,30] Br-F-ORH and TF-ORH were synthesized via Suzuki coupling and Knoevenagel condensation reaction, respectively.

Synthesis of Br-F-ORH: 5-Bromo-2-furaldehyde (0.84 g, 4.8 mmol) was dissolved in anhydrous chloroform (30 mL), and a few drops of piperidine and ORH (2.94 g, 12.0 mmol) were added. After refluxed and stirred for 5 min under an N_2 atmosphere, the reaction mixture was extracted with dichloromethane, washed with water, and dried over $MgSO_4$. After purification by column chromatography (dichloromethane: hexane = 1:1), the compound Br-F-ORH was obtained as a yellow solid (1.39 g, 72% yield). ^1H NMR (400 MHz, $CDCl_3$): δ (ppm) 7.35 (s, 1H), 6.76 (d, $J = 3.6$ Hz, 1H), 6.52 (d, $J = 3.6$, 1H), 4.09 (t, $J = 7.7$ Hz, 2H), 1.69 (m, 2H), 1.27 (m, 10H), 0.88 (t, $J = 6.9$ Hz, 3H).

Synthesis of TF-ORH: Degassed H_2O solution of potassium phosphate tribasic (K_3PO_4, 1 M, 7.2 mL) was added to 30 mL of tetrahydrofuran (THF) solution of Br-F-ORH (0.95 g, 2.36 mmol), B-T-ORH (1.10 g, 2.36 mmol), tri-tert-butylphos-
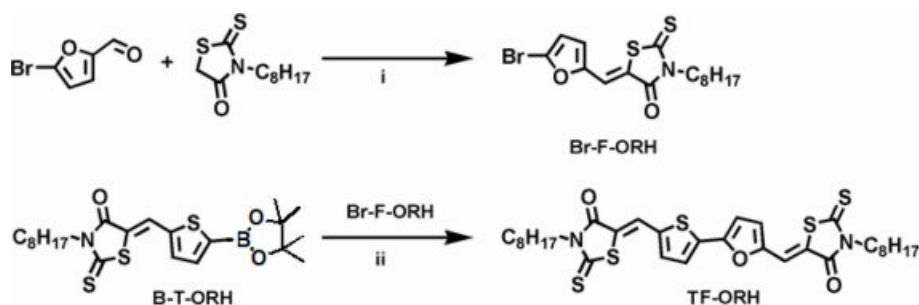
Scheme 1. The synthesis of TF-ORH. (i) Piperidine, chloroform, 5 min; (ii) Pd$_2$(dba)$_3$, K$_3$PO$_4$ (aq, 1 M), THF, reflux, N$_2$, 4 h.

phonium tetrafluoroborate (P(t-Bu)$_3$·HBF$_4$, 0.041 g, 0.14 mmol), and tris(dibenzylideneacetone)dipalladium(0) (Pd$_2$(dba)$_3$), 0.065 g, 0.07 mmol). After refluxed and stirred for 4 h under an N$_2$ atmosphere, the reaction mixture was extracted with dichloromethane, washed with water, and dried over MgSO$_4$. After recrystallized by methanol and purified by column chromatography (chloroform:hexane = 5:1), the final product of TF-ORH was obtained as a purple solid (0.25 g, 16% yield). ^{1}H NMR (400 MHz, CDCl$_3$): δ (ppm) 7.85 (d, 0.5 Hz, 1H), 7.53 (d, J = 4.0 Hz, 1H), 7.45 (s, 1H), 7.41 (d, J = 4.0, 0.5 Hz, 1H), 6.93 (d, J = 3.8 Hz, 1H) 6.84 (d, J = 3.8 Hz, 1H), 4.12 (m, 4H), 1.71 (m, 4H), 1.27 (m, 20H), 0.88 (t, J = 6.9 Hz, 6H). ^{13}C NMR (126 MHz, CDCl$_3$): δ (ppm) 193.99, 191.88, 167.64, 167.62, 152.39, 150.57, 138.88, 138.36, 134.94, 126.66, 124.38, 122.44, 122.11, 121.05, 116.85, 111.39, 45.18, 44.97, 31.99, 29.35, 27.24, 27.20, 27.00, 22.85, 14.31. Anal. Calc. for C$_{32}$H$_{40}$N$_2$O$_3$S$_5$: C, 58.15; H, 6.10; N, 4.24; S, 24.26. Found: C, 55.96; H, 5.88; N, 4.30; S, 23.88.

Results and Discussion

Synthesis and Thermal Properties. The nonfused A–D–A-type NFA, TF-ORH, was designed to have an asymmetric electron-donating core (TF) consisting of thiophene and furan, along with electron-withdrawing rhodanine (RH) groups at both ends, thus enabling TF-ORH to function as an acceptor in PSCs. The intermediate Br-F-ORH was synthesized through Knoevenagel condensation of bromo-2-furaldehyde and ORH in the presence of piperidine catalyst. TF-ORH was then obtained *via* the Suzuki coupling reaction of B-T-ORH and Br-F-ORH using a Pd$_2$(dba)$_3$ catalyst. The synthetic procedures are shown in Scheme 1. The purity of TF-ORH was verified by ^{1}H and ^{13}C NMR spectroscopy and elementary analyses (Figures S1-S2). TF-ORH was soluble in chloroform at a concentration sufficient for device fabrication.

Thermogravimetric analysis (TGA) and differential scanning calorimetry (DSC) were used to investigate the thermal properties of TF-ORH (Figure 1 and Table 1). TF-ORH showed a 5% loss of its initial weight at 383 °C, which was almost the same as T2-ORH,[30] indicating that its thermal stability is sufficient for device applications. In the DSC experiments, TF-ORH exhibited melting and crystallization temperatures of 164 and 145 °C, respectively, with both of these phase transition temperatures being higher than the corresponding values for T2-ORH (204 and 175 °C, respectively).[30] The introduction of furan also lowered the enthalpy changes of melting (ΔH_m) and crystallization (ΔH_{cryst}) from –70.0 and 68.8 J g^{-1}, respectively, for T2-ORH[18] to –45.3 and 44.6 J g^{-1}, respectively, for TF-ORH. Therefore, the asymmetric configuration created by introducing the furan moiety effectively lowered the molecular aggregation of the TF-ORH film, which is consistent with the higher solubility of TF-ORH than that of T2-ORH.
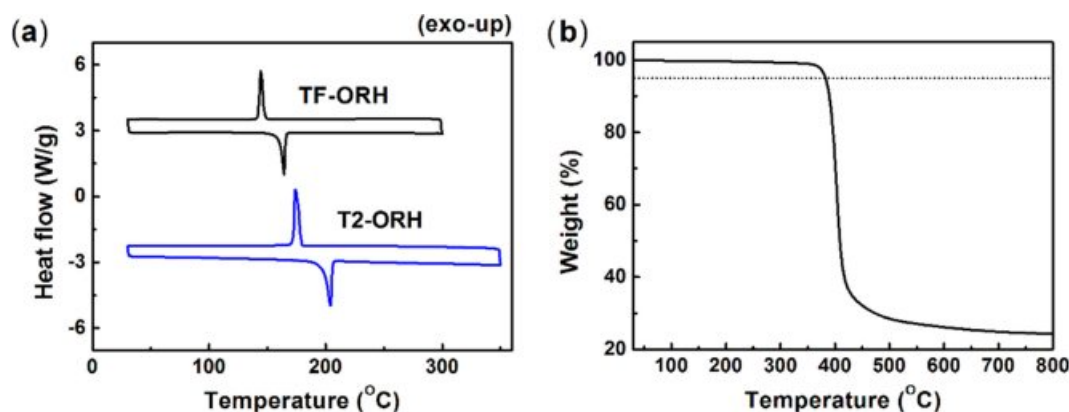

Figure 1. (a) DSC of TF-ORH and T2-ORH; (b) TGA of the TF-ORH.

Table 1. Thermal Properties of TF-ORH

	T_d (°C)[a]	T_m (°C)[b]	ΔH_m (J g^{-1})[c]	T_{cr} (°C)[d]	ΔH_{cryst} (J g^{-1})[e]
TF-ORH	383	164	–45.3	145	44.6

[a]Temperature showing 5% weight loss from the initial weight. [b]Temperature at the endothermal melting peak. [c]Enthalpic change at the endothermal melting peak. [d]Temperature at the exothermal crystallization peak. [e]Enthalpic change at the exothermal crystallization peak.

Optical and Electrochemical Properties. The UV–Vis absorption spectra of TF-ORH were measured and compared with those of T2-ORH and PTB7-Th (Figure 2(a)). The solution UV–Vis spectrum of TF-ORH showed an absorption maximum (λ_{max}) at 513 nm, almost the same as the λ_{max} of T2-ORH. The relatively short conjugation length (*i.e.*, two non-fused aromatic rings flanked by two RHs) of TF-ORH and T2-ORH resulted in a UV–Vis absorption at wavelengths below 600 nm. The λ_{max} of the TF-ORH film was 596 nm, which was red-shifted compared to the solution value, suggesting *J*-type aggregation. In contrary, the absorption of the as-cast T2-ORH film ($\lambda_{max} = 445$ nm) was blue-shifted relative to the solution value, consistent with *H*-aggregation.[30] In addition, the absorption of the T2-ORH film was red-shifted by annealing;[30] however, no absorption change was observed in the TF-ORH film (Figure S3). These findings suggest that the substitution of thiophene with furan changed the molecular packing behavior of the films The absorption spectrum of TF-ORH was complementary with that of the low bandgap polymer, PTB7-Th, which is beneficial for PSC applications. The optical energy bandgaps ($E_{g,opt}$)-calculated using the equation $E_{g,opt} = 1240/\lambda_{onset}$ (eV), where λ_{onset} is the absorption onset of the film-were 1.98 and 1.58 eV for TF-ORH and PTB7-Th, respectively.

The electrochemical properties were determined using cyclic voltammetry (CV). The films were prepared by dip-coating the small molecule solution onto the Pt working electrode, and the measurements were calibrated using the ferrocenium (Fc$^+$)/ferrocene (Fc) redox value of –4.8 eV as an external reference. The highest occupied molecular orbital (HOMO) and lowest unoccupied molecular orbital (LUMO) energy levels were estimated according to the empirical relationship $E_{HOMO} = -(E_{onset,ox} - E_{1/2,Fc} + 4.8)$ eV and $E_{LUMO} = -(E_{onset,red} - E_{1/2,Fc} + 4.8)$ eV, where $E_{onset,ox}$, $E_{onset,red}$, and $E_{1/2,Fc}$ are the onset potentials of oxidation and reduction, and half-wave potential of Fc/Fc$^+$ couple, respectively, assuming that the energy level of Fc is 4.8 eV below the vacuum level.[31,32] The HOMO and LUMO energy levels of TF-ORH were calculated to be –5.60 and –3.57 eV, respectively, resulting in an electrochemical energy bandgap ($E_{g,CV}$) of 2.03 eV. The energy diagrams of TF-ORH, T2-ORH, PTB7-Th are shown in Figure 2. The $E_{g,CV}$ of TF-ORH was slightly smaller than that of T2-ORH (2.07 eV). Compared to the energy levels of T2-ORH, the introduction of furan elevated the energy levels of the small molecule. A slightly stronger elevating effect of furan on the HOMO levels than on the LUMO levels resulted in the relatively smaller $E_{g,CV}$ of TF-ORH. In addition, when the polymer donor is PTB7-Th ($E_{HOMO} = -5.17$ eV and $E_{LUMO} = -3.50$ eV), the elevation of the energy levels on going from T2-ORH to TF-ORH reduced the energy offsets (ΔE_{LUMO} and ΔE_{HOMO}) between donor and acceptor. The ΔE_{LUMO} for the PTB7-Th:TF-ORH blend film was lowered to
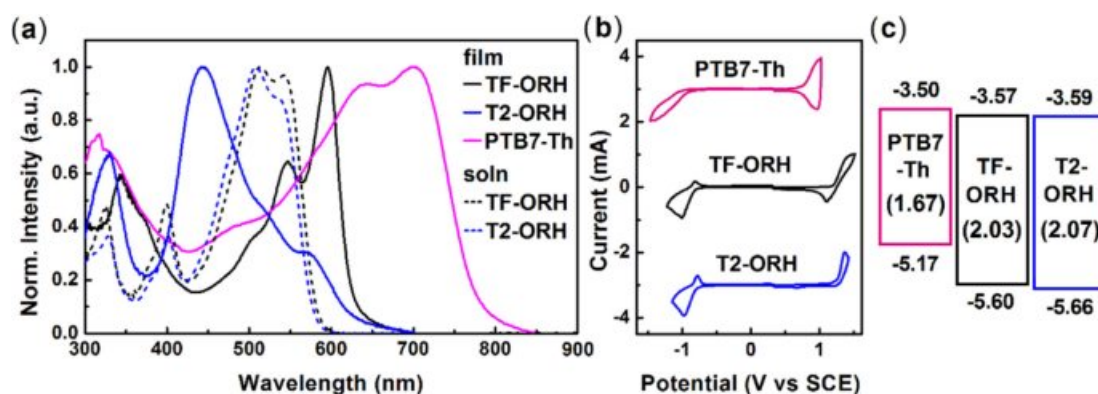

Figure 2. (a) UV-Vis absorption spectra; (b) CV; (c) energy diagram of the donor and acceptors used in this study.

Table 2. Physical Properties of TF-ORH and PTB7-Th

	E_{HOMO} (eV)[a]	E_{LUMO} (eV)[a]	$E_{g,CV}$ (eV)[b]	λ_{max} (soln) (nm)[c]	λ_{max} (film) (nm)[c]	$E_{g,opt}$ (eV)[d]
TF-ORH	–5.60	-3.57	2.03	513	596	1.98
PTB7-Th	–5.17	-3.50	1.67	-	700	1.58

[a]$E_{HOMO} = -(E_{onset,ox} - E_{1/2,Fc} + 4.8)$, $E_{LUMO} = -(E_{onset,red} - E_{1/2,Fc} + 4.8)$. [b]$E_{g,CV} = E_{LUMO} - E_{HOMO}$. [c]Absorption maxima in chloroform solution and film. [d]$E_{g,opt} = 1240/\lambda_{onset}$ (eV).

0.07 eV, while the ΔE_{LUMO} value for the PTB7-Th:T2-ORH film was slightly larger than that of the PTB7-Th:TF-ORH film but still smaller than 0.3 eV. Previous studies have indicated that HOMO and LUMO energy level offsets greater than 0.3 eV are required for efficient energy transfer between the donor and acceptor.[33] However, recent investigations have shown that effective energy transfer can also occur in devices with energy offsets below 0.3 eV in which the smaller offset leads to a small E_{loss}, allowing the maximum possible open-circuit voltage (V_{OC}) to be achieved in a given D:A system.[34] In our previous study, a small E_{loss} of ~0.5 eV and thus a high V_{OC} of 1.05 eV were achieved in a D:A system in which the ΔE_{LUMO} between donor and acceptor was smaller than 0.1 eV.[18] Table 2 summarized the physical properties of TF-ORH and PTB7-Th.

Organic Photovoltaic Properties. The PSCs were fabricated with the inverted device structure: ITO/ZnO NPs/PEIE/ active layer/MoO$_x$/Ag. An active layer was prepared consisting of PTB7-Th and TF-ORH as donor and acceptor, respectively. PTB7-Th and TF-ORH were dissolved in chloroform in a ratio of 1:2 at a total solids concentration of 15 mg mL^{-1}. The current density–voltage (J–V) and external quantum efficiency (EQE) curves obtained under AM 1.5G illumination (100 mW cm^{-2}) are shown in Figure 3. The photovoltaic properties of the PTB7-Th:TF-ORH device are summarized in Table 3.

The as-cast device exhibited a PCE of 0.49% with a V_{OC} of 0.87 V, a short-circuit current (J_{SC}) of 1.75 mA cm^{-2}, and a fill factor (FF) of 32%. When 1.0 vol% diiodoctane (DIO) was added to the chloroform solvent as an additive, the device performance was increased upto 1.21% owing to the increased J_{SC} (3.21 mA cm^{-2}) and FF (43%). Moreover, The PTB7-Th:TF-ORH device exhibited a broad EQE profile from 350–750 nm. The two EQE peaks centered at 540 and 720 nm corresponded to the UV–Vis absorption maxima of TF-ORH (λ_{max} = 445 nm) and PTB7-Th (λ_{max} = 700 nm), respectively, indicative of charge generation via both hole and electron transfer.[17,30]

The V_{OC} of the PTB7-Th:TF-ORH device was 0.88 V, which was lower than that of the PTB7-Th:T2-ORH device (1.04 V), but comparable with those reported for high efficiency devices[35] (*e.g.*, PTB7-Th:ITIC (V_{OC} = 0.83 V)).[30] The relatively high V_{OC} of the PTB7-Th:TF-ORH device can be explained by the high-lying LUMO energy level of TF-ORH and the relatively low E_{loss} of 0.70 eV, calculated using the following equation:[36] $E_{loss} = E_{g,opt}$ (PTB7-Th)-eV_{OC}. According to the literature,[36] few studies have achieved E_{loss} values below 0.7 eV for devices prepared using a low bandgap (<1.6 eV) donor polymer and a wide bandgap (>1.8 eV) NFA.
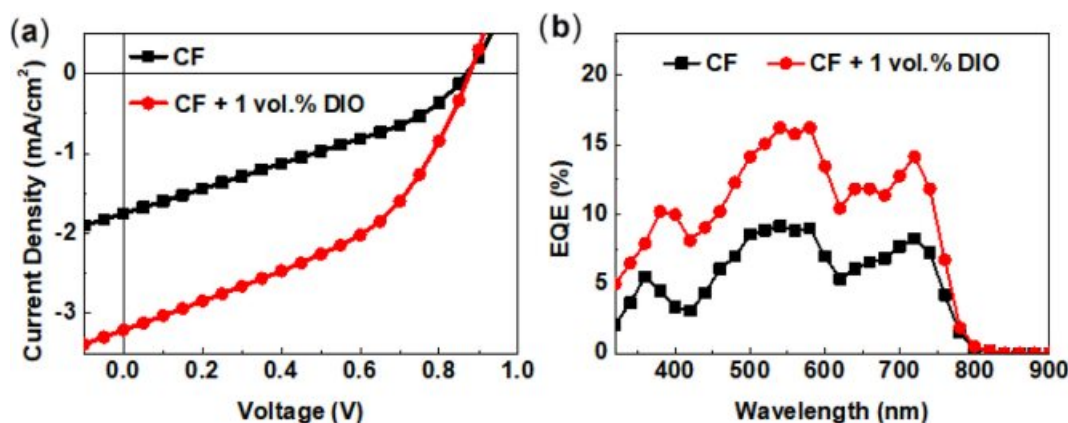

Figure 3. (a) J–V; (b) EQE curves of the PTB7-Th:TF-ORH PSCs.

Table 3. Photovoltaic Properties of the PSC Devices[a,b]

Solvent	V_{OC} (V)	J_{SC} (mA cm^{-2})	FF (%)	PCE (%)
CF	0.87 (0.87 ± 0.01)	1.75 (1.72)[c] (1.59 ± 0.17)	32 (31 ± 2)	0.49 (0.34 ± 0.16)
CF (1 vol% DIO)	0.88 (0.87 ± 0.01)	3.21 (3.10)[c] (3.11 ± 0.11)	43 (42 ± 1)	1.21 (1.07 ± 0.15)

[a]ITO/ZnO NPs/PEIE/PTB7-Th:TF-ORH/MoO$_x$/Ag. [b]The values in parenthesis are average photovoltaic properties obtained from over 10 devices. [c]J_{SC} values in parenthesis calculated from the EQE spectra.

Conclusions

We synthesized a nonfused NFA with a simple structure, TF-ORH, containing a nonfused asymmetrical thiophene-furan core flanked by octyl-substituted rhodanine end groups. TF-ORH had sufficient solubility and thermal stability for PSC applications, and exhibited physical properties complementary to those of the low bandgap polymer donor PTB7-Th. A PSC fabricated using PTB7-Th:TF-ORH blend film exhibited a PCE of 1.21% with a V_{OC} of 0.88 V and a small E_{loss} of 0.70 eV.

Supporting Information: Information is available regarding synthesis, ^{1}H and ^{13}C NMR spectra, physical measurement, and device fabrication.

References

1. S. Park, H. Ahn, J.-y. Kim, J. B. Park, J. Kim, S. H. Im, and H. J. Son, *ACS Energy Lett.*, **5**, 170 (2020).
2. L. Hong, H. Yao, Z. Wu, Y. Cui, T. Zhang, Y. Xu, R. Yu, Q. Liao, B. Gao, K. Xian, H. Y. Woo, Z. Ge, and J. Hou, *Adv. Mater.*, **31**, 1903441 (2019).
3. K. Kranthiraja, H.-Y. Park, K. Gunasekar, W.-T. Park, Y.-Y. Noh, Y.-S. Gal, J. H. Moon, J. Y. Lee, and S.-H. Jin, *Macromol. Res.*, **26**, 500 (2018).
4. S. Nho, D. H. Kim, S. Park, H. N. Tran, B. Lim, and S. Cho, *Dyes Pigm.*, **151**, 272 (2018).
5. H. Sun, T. Liu, J. Yu, T.-K. Lau, G. Zhang, Y. Zhang, M. Su, Y. Tang, R. Ma, B. Liu, J. Liang, K. Feng, X. Lu, X. Guo, F. Gao, and H. Yan, *Energy Environ. Sci.*, **12**, 3328 (2019).
6. Y. Lin and X. Zhan, *Mater. Horiz.*, **1**, 470 (2014).
7. Y.-C. Lin, Y.-J. Lu, C.-S. Tsao, A. Saeki, J.-X. Li, C.-H. Chen, H.-C. Wang, H.-C. Chen, D. Meng, K.-H. Wu, Y. Yang, and K.-H. Wei, *J. Mater. Chem. A*, **7**, 3072 (2019).
8. J. Wang, J. Zhang, Y. Xiao, T. Xiao, R. Zhu, C. Yan, Y. Fu, G. Lu, X. Lu, S. R. Marder, and X. Zhan, *J. Am. Chem. Soc.*, **140**, 9140 (2018).
9. J. Yuan, Y. Zhang, L. Zhou, G. Zhang, H.-L. Yip, T.-K. Lau, X. Lu, C. Zhu, H. Peng, P. A. Johnson, M. Leclerc, Y. Cao, J. Ulanski, Y. Li, and Y. Zou, *Joule*, **3**, 1140 (2019).
10. R. Ma, T. Liu, Z. Luo, Q. Guo, Y. Xiao, Y. Chen, X. Li, S. Luo,

X. Lu, M. Zhang, Y. Li, and H. Yan, *Sci. China Chem.*, **63**, 325 (2020).
11. H. Yao, Y. Cui, D. Qian, C. S. Ponseca, A. Honarfar, Y. Xu, J. Xin, Z. Chen, L. Hong, B. Gao, R. Yu, Y. Zu, W. Ma, P. Chabera, T. Pullerits, A. Yartsev, F. Gao, and J. Hou, *J. Am. Chem. Soc.*, **141**, 7743 (2019).
12. C. Li, Y. Xie, B. Fan, G. Han, Y. Yi, and Y. Sun, *J. Mater. Chem. C*, **6**, 4873 (2018).
13. J. Song, C. Li, L. Ye, C. Koh, Y. Cai, D. Wei, H. Y. Woo, and Y. Sun, *J. Mater. Chem. A*, **6**, 18847 (2018).
14. C. Li, J. Song, L. Ye, C. Koh, K. Weng, H. Fu, Y. Cai, Y. Xie, D. Wei, H. Y. Woo, and Y. Sun, *Solar RRL*, **3**, 1800246 (2019).
15. X. Li, C. Li, L. Ye, K. Weng, H. Fu, H. S. Ryu, D. Wei, X. Sun, H. Y. Woo, and Y. Sun, *J. Mater. Chem. A*, **7**, 19348 (2019).
16. C. Li, H. Fu, T. Xia, and Y. Sun, *Adv. Energy Mater.*, **9**, 1900999 (2019).
17. S. Feng, C. E. Zhang, Y. Liu, Z. Bi, Z. Zhang, X. Xu, W. Ma, and Z. Bo, *Adv. Mater.*, **29**, 1703527 (2017).
18. T. Lee, S. Oh, S. Rasool, C. E. Song, D. Kim, S. K. Lee, W. S. Shin, and E. Lim, *J. Mater. Chem. A*, **8**, 10318 (2020).
19. Y. M. Kim, E. Lim, I.-N. Kang, B.-J. Jung, J. Lee, B. W. Koo, L.-M. Do, and H.-K. Shim, *Macromolecules*, **39**, 4081 (2006).
20. H. J. Lee, G. E. Park, S. Choi, D. H. Lee, H. A. Um, J. Shin, M. J. Cho, and D. H. Choi, *Polymer*, **94**, 43 (2016).
21. T. W. Lee, D. H. Lee, J. Shin, M. J. Cho, and D. H. Choi, *Polym. Chem.*, **6**, 1777 (2015).
22. P. Ye, Y. Chen, J. Wu, X. Wu, Y. Xu, Z. Li, S. Hong, M. Sun, A. Peng, and H. Huang, *Mater. Chem. Front.*, **3**, 64 (2019).
23. A. Mahmood, J. Hu, A. Tang, F. Chen, X. Wang, and E. Zhou, *Dyes Pigm.*, **149**, 470 (2018).
24. P. Ye, Y. Chen, J. Wu, X. Wu, S. Yu, W. Xing, Q. Liu, X. Jia, A. Peng, and H. Huang, *J. Mater. Chem. C*, **5**, 12591 (2017).
25. Suman, A. Bagui, R. Datt, V. Gupta, and S. P. Singh, *Chem. Commun.*, **53**, 12790 (2017).
26. Suman, A. Bagui, A. Garg, B. Tyagi, V. Gupta, and S. P. Singh, *Chem. Commun.*, **54**, 4001 (2018).
27. Y. Eom, C. E. Song, W. S. Shin, S. K. Lee, and E. Lim, *J. Ind. Eng. Chem.*, **45**, 338 (2017).
28. C. Li, T. Xia, J. Song, H. Fu, H. S. Ryu, K. Weng, L. Ye, H. Y. Woo, and Y. Sun, *J. Mater. Chem. A*, **7**, 1435 (2019).
29. C. Li, J. Song, Y. Cai, G. Han, W. Zheng, Y. Yi, H. S. Ryu, H. Y. Woo, and Y. Sun, *J. Energy Chem.*, **40**, 144 (2020).
30. T. Lee, Y. Eom, C. E. Song, I. H. Jung, D. Kim, S. K. Lee, W. S. Shin, and E. Lim, *Adv. Energy Mater.*, **9**, 1804021 (2019).
31. O. Kwon, J. Jo, B. Walker, G. C. Bazan, and J. H. Seo, *J. Mater. Chem. A*, **1**, 7118 (2013).
32. D. Liu, B. Kan, X. Ke, N. Zheng, Z. Xie, D. Lu, and Y. Liu, *Adv. Energy Mater.*, **8**, 1801618 (2018).
33. M. C. Scharber, D. Mühlbacher, M. Koppe, P. Denk, C. Waldauf, A. J. Heeger, and C. J. Brabec, *Adv. Mater.*, **18**, 789 (2006).
34. T. Zhang, X. Zhao, D. Yang, Y. Tian, and X. Yang, *Adv. Energy Mater.*, **8**, 1701691 (2018).
35. Suman and S. P. Singh, *J. Mater. Chem. A*, **7**, 22701 (2019).
36. J. Zhang, L. Zhu, and Z. Wei, *Small Methods*, **1**, 1700258 (2017).